Charge-density-wave transport in quasi-one-dimensional conductors. II. ac-dc interference phenomena

R. E. Thorne, W. G. Lyons, J. W. Lyding, and J. R. Tucker
Department of Electrical and Computer Engineering, Coordinated Science Laboratory, and Materials Research Laboratory, University of Illinois at Urbana-Champaign, Urbana, Illinois 61801

John Bardeen
Department of Physics, University of Illinois at Urbana-Champaign, Urbana, Illinois 61801
(Received 29 August 1986)

We present a detailed experimental study of ac-dc interference phenomena in charge-density-wave (CDW) transport. Harmonic and subharmonic "steps" of constant CDW current are observed when ac and dc voltages are applied together, and the widths of these steps exhibit Bessel-like oscillations as a function of both ac amplitude and frequency. We now observe similar oscillations in the dc threshold field, and thereby complete the analogy between these phenomena and similar effects in Josephson junctions. By minimizing crystal defects and contact effects, we have obtained complete harmonic and subharmonic phase locking in very long $NbSe_3$ crystals under a broad range of conditions, including cases where the total time-dependent voltage remains above the dc threshold V_T. We analyze our experimental results with a single-coordinate model used previously to account for subharmonic steps. It is based on the tunneling theory and assumes CDW motion in a highly nonsinusoidal pinning potential. This model provides an excellent and semiquantitative account of all our results; it also provides a detailed interpretation of interference features observed in the ac conductance, electric-field-induced anomalies observed in the CDW elastic response, and the inductive loops observed in phase-space plots of the CDW's response to ac fields. The quality of the agreement provides strong evidence both for an effective pinning potential of the proposed form and for a single-degree-of-freedom description of CDW transport.

I. INTRODUCTION

Current oscillation and ac-dc interference phenomena provide the most striking manifestations of the interaction between sliding charge-density waves (CDW's) and impurities. To minimize its impurity interaction energy, the CDW deforms,[1] thereby losing its translational symmetry and becoming pinned to the lattice. Since displacements of the CDW by integral numbers of wavelengths do not change this interaction, the impurity pinning potential is expected to be periodic in the displacement. As discussed in the preceding paper[2] (hereafter referred to as I), when a dc electric field is applied, the CDW's velocity is periodically modulated by the pinning force, resulting in current oscillations. The Fourier spectrum of these current oscillations consists of a fundamental peak, whose frequency ω_n is proportional to the dc CDW current, and a rich array of higher harmonics.

When dc and ac fields are applied together, $V(t)=V_{\rm dc}+V_{\rm ac}\cos(\omega t)$, striking interference phenomena are observed. The dc I-V characteristic exhibits steps where the dc CDW current remains constant while the dc voltage varies.[3] The width of these steps depends on the frequency and amplitude of the ac field.[4] Analogous features are observed in the response of resistively-shunted Josephson junctions;[5] the steps in the CDW I-V characteristic are thus sometimes referred to as Shapiro steps. For applied fields such that steps are observed in the dc I-V characteristic, the real part of the ac conductance exhibits sharp positive jumps and the imaginary part exhibits its negative ("inductive") dips.[6] Anomalies associated with applied ac and dc fields are also observed in the elastic response.[7] All of these phenomena are due to interference or phase locking of the internal CDW frequency ω_n with the externally applied frequency ω. Both harmonic features, for which $\omega_n/\omega=p$, and subharmonic features,[8] for which $\omega_n/\omega=p/q(\neq r)$, where p, q, and r are integers, are observed.

In order to account for subharmonic steps in the dc I-V characteristic, a simple model was proposed[9] in which the only variables are the space-average CDW phase and a phase-dependent pinning potential. Good agreement was obtained between theory and measurements performed at the University of California at Los Angeles (UCLA) of subharmonic steps in $NbSe_3$. However, the comparison was made only for a single ac frequency and amplitude, and experimental parameters important to the theoretical analysis were not available.

Paper I presented results of our detailed measurements of the current oscillations. These measurements indicated that the effective pinning potential is highly nonsinusoidal, and that its magnitude and form remain approximately independent of electric field even at very high fields. A single-coordinate model, motivated by the tunneling theory of CDW depinning, was seen to account qualitatively for these findings. In this paper, we present an extensive study of ac-dc interference phenomena in CDW systems. We show that all qualitative features of these phenomena—steps in the dc I-V characteristic, jumps and dips in the ac conductance, oscillations in the dc threshold, and anomalies in the elastic response—can also be understood using the same single-coordinate model that accounts for the current oscillations. This constitutes strong evidence that the CDW's interaction with impurities may be described, to good approximation, in terms of a periodic pinning potential of the general form proposed[10] within the context of the tunneling theory and a single effective degree of freedom.

II. EXPERIMENTAL METHODS AND RESULTS

The material of choice for study ac-dc interference phenomena is again $NbSe_3$, because it exhibits the most coherent response of any CDW material. Interference phenomena in the dc I-V characteristic and in the ac conductance were measured as a function of the amplitude and frequency of an applied sinusoidal voltage. $NbSe_3$ crystals of modest purity (with a residual resistivity ratio of 130) were mounted in a two-probe configuration on a 50-Ω microstrip with silver paste and placed in an open-cycle refrigeration system with a helium exchange gas. ac and dc voltages were applied using a Marconi 2022 signal generator and a Systron-Donner M107 precision dc voltage source, respectively. Rather than measure the dc I-V characteristic directly, the differential resistance dV/dI was measured versus dc voltage using a PAR 5301 lock-in amplifier. The steps in the I-V characteristic appear as peaks in dV/dI. The ac conductance was measured using a Rhode and Schwarz ZPV vector analyzer. All measurements were automated through the use of an IBM PC/AT computer.

$NbSe_3$ undergoes two CDW transitions, the first at 145 K and the second at 59 K. The CDW which forms below the second transition is in general more coherent, resulting in sharper and more clearly defined interference features. In spite of this, we chose to perform our measurements at 120 K, on the CDW which forms below the first transition. This choice was made for two reasons. First, instrumental and background noise perturb the CDW, leading to intermittent loss of phase lock and rounding of the interference features. Since the width of the interference features in voltage is much larger for the first CDW, these effects are less important. Second, below the lower transition both CDW's are present; both contribute to the ac conductance and, at sufficiently high dc fields, to the dc conductance. This greatly complicates the interpretation of the measurements, and makes it impossible to determine the parameters required for a detailed comparison with theory.

As discussed in paper I, most theories of CDW transport describe only the CDW's interaction with randomly distributed impurities and presume CDW motion with a unique time-average velocity. Real materials exhibit a variety of defects which, together with contact effects, result in nonuniform current and velocity distributions. These defects and velocity distributions can play a determining role in the decay of transient "ringing" in the voltage response to current pulses and in broadband noise generation, as shown in paper I. They also affect the form of the interference peaks observed here in the differential resistance. In highly coherent samples, the harmonic and some low-order subharmonic peaks have flat tops where dV/dI is equal to the normal electron resistance which shunts the CDW,[11] as in Fig. 1. The dc CDW current is thus constant for some range of applied dc voltage, so that phase locking to the external ac field is complete. In less coherent samples, the peaks in dV/dI are rounded and do not reach the normal electron resistance; the CDW current varies somewhat on the step, and the locking is incomplete. A recent experimental study[12] has concluded that the ac-induced CDW velocity coherence length, defined as the maximum sample length for which complete phase locking can be observed, is less than 1 mm for the CDW which forms below 59 K in $NbSe_3$. Figure 1 shows the differential resistance measured in the presence of an applied ac voltage in a 2.8-mm-long $NbSe_3$ sample on the upper CDW transition. Complete phase locking is observed for the 1/1 harmonic step as well as for the 1/2 and 1/3 subharmonic steps. Our results for all samples clearly indicate that complete phase locking occurs only if the distribution of time-average CDW velocities within the crystal is sufficiently narrow, and that this distribution results primarily from crystal defects and contact effects. As discussed in paper I, the "intrinsic" CDW response appears to be characterized by essentially perfect velocity coherence. With improvements in experimental technique, it should be possible to obtain complete phase locking in samples of arbitrary length; the ac-induced velocity coherence length thus would seem to have no fundamental physical significance. Unless otherwise stated, all measurements reported in this paper were performed on the sample of Fig. 1. To facilitate comparisons with theory, Table I gives the important experimental parameters of this sample.

We shall first discuss the interference features in the dc I-V characteristics observed when a voltage $V(t) = V_{dc} + V_{ac}\cos\omega t$ is applied. In particular, we are interested in the variation of the width of the steps (peaks in

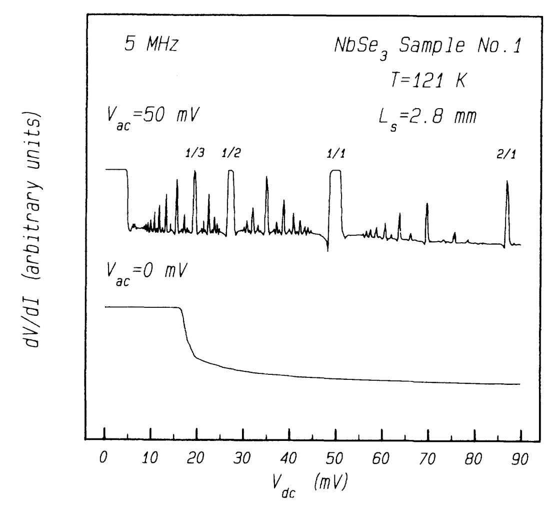

FIG. 1 Differential resistance of a 2.8-mm-long $NbSe_3$ sample at 121 K, measured in the presence of a 5-MHz, 50-mV peak ac voltage. Complete locking is observed for the 1/1, 1/2, and 1/3 peaks.

TABLE I. Experimental parameters of $NbSe_3$ sample No. 1 at $T = 121$ K. The parameters G_a, G_b, and V_0 describe the Zener fit to the dc I-V characteristic: $I_{CDW} = G_a V + G_b V \exp(-V_0/V)$. The classical crossover frequency ω_{co} was obtained from the measured peak in the imaginary part of the ac conductance. The room-temperature resistance was 570 Ω.

L_s (mm)	2.8
G_a (mΩ^{-1})	3.18
G_b (mΩ^{-1})	0.816
V_T (mV)	15.8
V_0 (mV)	32.4
I_{CDW}/v_n (μA/MHz)	4.5
$\omega_{co}/2\pi$ (MHz)	12

dV/dI) with the frequency ω and amplitude V_{ac} of the applied ac voltage. Since most peaks in dV/dI do not exhibit complete locking, the step width was calculated as $\delta V \equiv \int (dV/dI) dI$. Figure 2 shows the measured step widths of the 1/1 through 1/5 steps versus ac amplitude

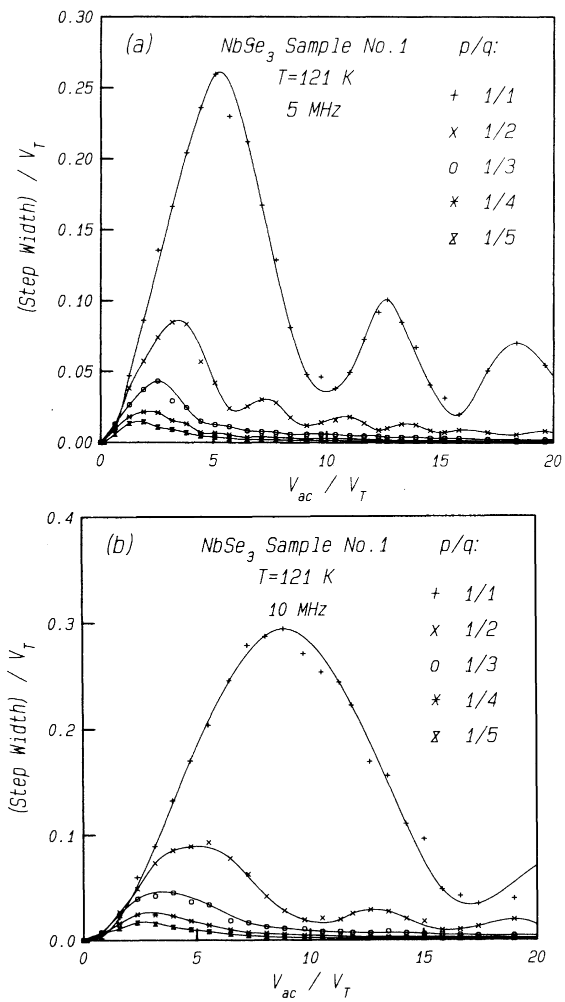

FIG. 2. Widths of selected steps in the dc I-V characteristic vs peak ac amplitude for applied ac frequencies of (a) 5 MHz and (b) 10 MHz. The period of the oscillations with ac amplitude varies as $1/q$ for the p/q step. The solid lines are guides to the eye.

for ac frequencies of 5 and 10 MHz. Several features are noteworthy. First, both the harmonic and subharmonic step widths exhibit Bessel-like oscillations, with the envelope of the oscillations decreasing with increasing ac amplitude. Second, the maximum step width versus ac amplitude decreases with increasing subharmonic order q. Third, the period of the oscillations varies with increasing q as $1/q$. These general features were observed at all frequencies, although both the harmonic and subharmonic oscillations were less pronounced at lower frequencies (e.g., 500 kHz).

Figure 3 shows the variation of the width of the 1/1, 2/1, and 3/1 harmonic steps with ac amplitude for an applied ac frequency of 2 MHz. The initial increase in step width becomes more gradual and the maximum step width becomes smaller with increasing harmonic order p. However, for large V_{ac} the amplitudes of the oscillations are approximately the same, and the phase of the oscillations for even p steps is opposite to that for odd p.

Figure 4 shows the width of the 1/1 step as a function of ac amplitude for applied ac frequencies between 500 kHz and 20 MHz. The period of the oscillations with ac amplitude is roughly proportional to the frequency. The maximum step width increases rapidly with increasing frequency at low frequencies. At high frequencies, however, the maximum step width saturates to a value of about one-third the dc threshold voltage.

An applied ac voltage suppresses the dc threshold field for CDW conduction. Previous studies by our group[13] and by others[6,14,15] indicated that the dc threshold decreases smoothly to zero with increasing ac amplitude, and that the amplitude required in order to achieve a given change in the dc threshold increases approximately linearly with ac frequency. Figure 5 shows the measured dc threshold field as a function of ac amplitude for ac frequencies between 2 and 20 MHz. Threshold oscillations with ac amplitude are clearly observed. Further, the gen-

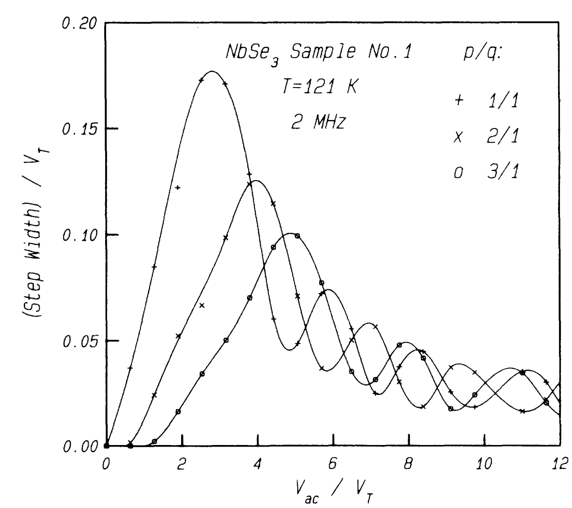

FIG. 3. Widths of the 1/1, 2/1, and 3/1 harmonic steps vs peak ac amplitude for an applied ac frequency of 2 MHz. For large ac voltages, the step width oscillations for different p values have nearly the same magnitude, and the phase of the even and odd p oscillations differ by 180°. The solid lines are guides to the eye.

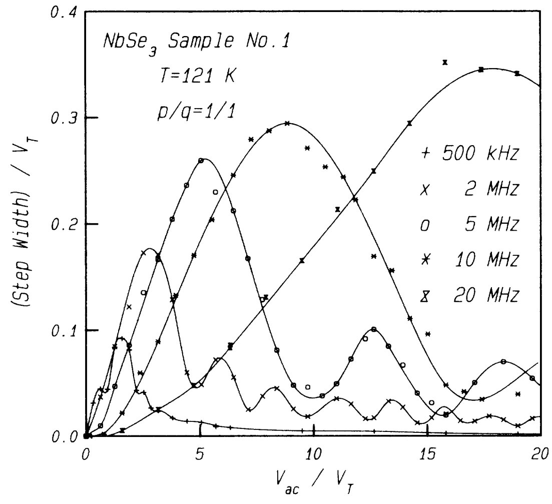

FIG. 4. Width of the 1/1 step vs ac amplitude for several applied ac frequencies. The periods of the oscillations with ac amplitude are roughly proportional to the ac frequency. The maximum magnitude of the oscillations increases at low frequencies but saturates at high frequencies. The solid lines are guides to the eye.

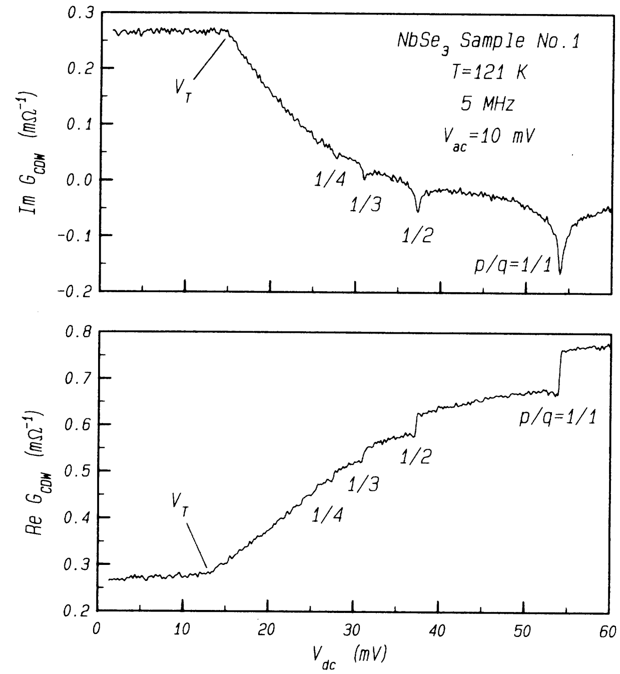

FIG. 6. Real and imaginary components of the bias-dependent ac conductance measured using a 5-MHz, 10-mV peak ac voltage. Several harmonic and subharmonic interference features are visible.

eral behavior is very similar to that of the steps in the I-V characteristic: the period and amplitude of the oscillations both increase with increasing frequency. Samples of exceptional coherence are required in order to see these oscillations because of their small amplitude; we did not observe dc threshold oscillations previously because our samples were not of sufficient quality. The analogy between ac-induced interference features seen in the dc I-V characteristic of CDW systems and those in Josephson junctions is now complete.

We shall now discuss the interference features observed in the ac conductance. Figure 6 shows the CDW conductance measured using a small amplitude ac voltage at a frequency of 5 MHz. As noted previously,[6] the real part of the ac conductance exhibits abrupt jumps and the imaginary part exhibits sharp negative ("inductive") dips at the same dc biases where steps are observed on the I-V characteristic. Several features corresponding to subharmonic phase locking are clearly visible, illustrating the exceptional coherence of this sample. Note that curvature in the conductance is observed adjacent to the steps even for biases at which complete locking does not occur. The small signal bias-dependent ac conductance measured at frequencies of 2, 5, and 10 MHz is shown in Fig. 7. As expected, the interference features move to larger dc biases with increasing ac frequency. The significance of any variation in the size of the features with frequency is not clear, because for small ac amplitudes the phase-locked width is comparable to the distribution of velocities within this crystal.

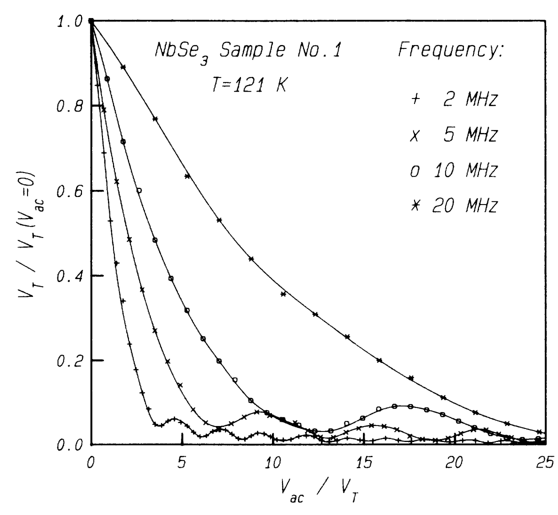

FIG. 5. The dc threshold voltage vs ac amplitude for several applied ac frequencies. The period of the oscillations with ac amplitude is roughly proportional to the ac frequency. The solid lines are guides to the eye.

More interesting, and somewhat surprising, results are obtained when the bias-dependent ac conductance is measured versus ac amplitude. As shown in Fig. 8, the slope of the jumps in ReG_{CDW} becomes more gradual with increasing ac amplitude, and at very large amplitudes the jumps disappear completely. Similarly, the inductive dips in Im G_{CDW} become shallow and broad with increasing ac amplitude. However, for ac amplitudes near that which produces the maximum step width in the I-V characteristic, the 1/1 "dip" of ImG_{CDW} actually becomes slightly positive (arrow in Fig. 8), indicating capacitive behavior. Similar results were obtained at other frequencies and for subharmonic dips. These interference features in the ac

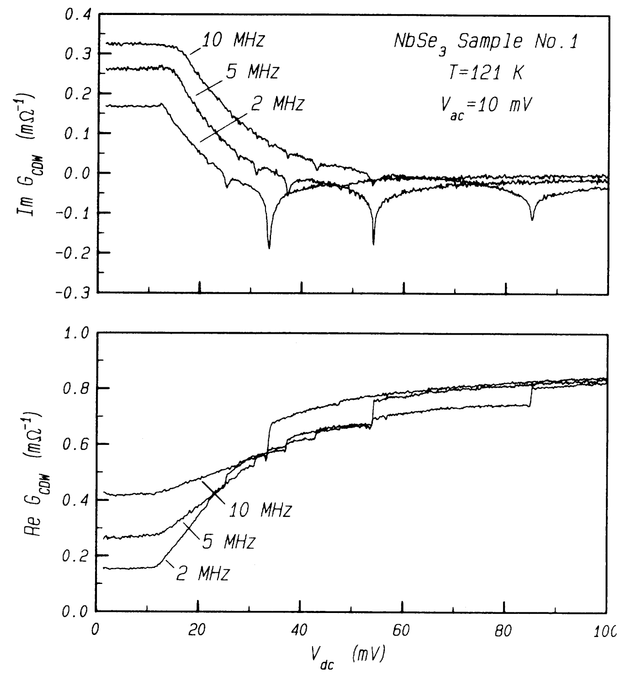

FIG. 7. Real and imaginary components of the bias-dependent ac conductance measured at 2, 5, and 10 MHz using a 10-mV peak ac voltage. The largest interference feature at each frequency corresponds to $p/q=1/1$.

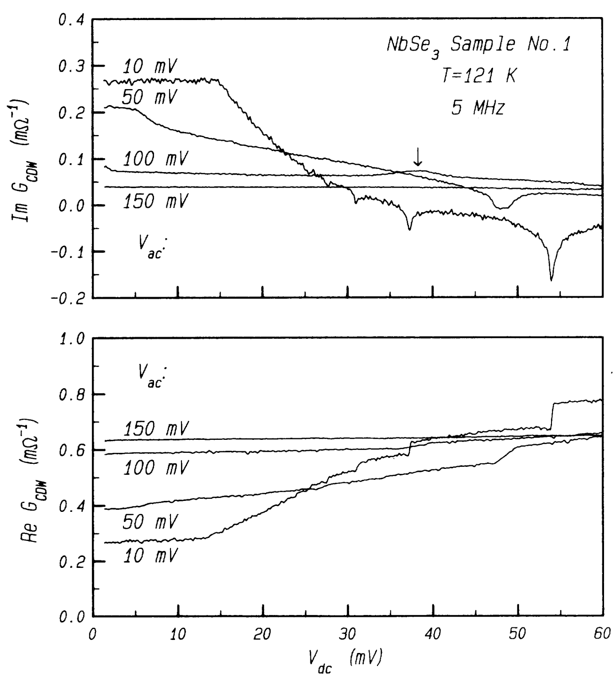

FIG. 8. Real and imaginary components of the bias-dependent ac conductance measured at 5 MHz using ac amplitudes of 10, 50, 100, and 150 mV. The largest interference feature at each ac amplitude corresponds to $p/q=1/1$. Large negative dips in $\mathrm{Im}\,G_{\mathrm{CDW}}$ which are observed for small ac amplitudes vanish for large ac amplitudes. At 100 mV, the polarity of the 1/1 interference feature in $\mathrm{Im}\,G_{\mathrm{CDW}}$ (indicated by the arrow) has become positive.

conductance are observed to vanish at relatively modest ac voltages—on the order of that corresponding to the first minimum in step width versus ac amplitude.

III. ANALYSIS AND DISCUSSION

Oscillations in response to a dc bias and interference phenomena in response to combined ac and dc excitations are also observed in resistively shunted Josephson junctions. The analogy with Josephson junctions has thus been used extensively[6] in the analysis of CDW interference phenomena. In the resistively shunted junction (RSJ) model,[16] the phase difference θ between the macroscopic wave functions on opposite sides of the junction is described by a differential equation of the form

$$\alpha(d^2\theta/dt^2)+\beta(d\theta/dt)+\mathcal{V}'(\theta)=F(t)\ , \tag{1}$$

where $\mathcal{V}'(\theta)=I_c\sin\theta$ represents an internal force term periodic in the phase θ, and $F(t)=I(t)$ is the driving force due to the applied current. In converting Eq. (1) to CDW systems, the roles of current and voltage are interchanged, and $F(t)$ becomes the applied voltage $V(t)$. The internal force term, which is now equal to the derivative of the pinning potential, is often assumed to be $\mathcal{V}'(\theta)=V_T\sin\theta$. Inertial effects are negligible at frequencies of up to several hundred megahertz,[17] so that the first term in Eq. (1) can be neglected. The resulting equation of motion, which describes the rigid overdamped oscillator (ODO) model,[18,19] may then be written as

$$d\theta/dt=\omega_{\mathrm{co}}(V/V_T-\sin\theta)\ , \tag{2}$$

where ω_{co} is called the classical crossover frequency and V_T is the dc threshold voltage in the absence of applied ac fields. This equation accounts qualitatively for the presence of current oscillations and harmonic interference features. Subharmonic features are not predicted,[20] however, in clear disagreement with experiment. Furthermore, as discussed in paper I, model parameters deduced from different experiments do not satisfy the predicted relations. As a result, when measured parameters are used in Eq. (2) to calculate the widths of the harmonic steps in the I-V characteristic, the predicted step sizes oscillate almost an order of magnitude more rapidly with ac amplitude than is observed experimentally. Zettl and Grüner[6] reported agreement between the predictions of Eq. (2) and measured oscillations of the Shapiro steps by adjusting the values of the threshold voltage to compensate this order of magnitude discrepancy.

In order to analyze the ac-induced steps in the dc I-V characteristic, we adopt a simple and very general approach[9] similar to the one used by Shapiro.[5] We believe that it describes the essential physics of phase locking. The CDW current can in general be written in the form $I_{\mathrm{CDW}}=f(V_{\mathrm{eff}})$, where f is a functional of the effective force $V_{\mathrm{eff}}=V(t)-V_M\mathcal{V}'(\theta)$. Here V_M is the maximum magnitude of the periodic pinning force and $\max|\mathcal{V}'(\theta)|=1$. Internal degrees of freedom result in a CDW phase which varies with both space and time; we shall use a single coordinate description, so that $\theta(t)$ refers to the space-average phase. The widths of the steps of constant current may then be estimated without detailed knowledge of $f(V_{\text{eff}})$ by assuming that the dc CDW current depends only upon the time-average value of V_{eff}, which is calculated by assuming a specific form for the pinning potential $\mathscr{V}(\theta)$. For a CDW biased with a superposition of a dc and an ac current,

$$d\theta/dt = -\omega_d + \omega_1 \cos(\omega t) , \tag{3}$$

so that

$$\theta(t) = -\omega_d t + (\omega_1/\omega)\sin(\omega t) + \theta_0 . \tag{4}$$

Here ω_d is the average drift frequency, ω_1 is proportional to the amplitude of the ac current, and θ_0 is a constant of integration. The shape of the pinning potential may be Fourier analyzed in the form

$$\mathscr{V}(\theta) = a_0/2 + \sum_{q=1}^{\infty} a_q \cos(q\alpha\theta) , \tag{5}$$

where $\alpha = 1$ or 2 for pinning periodicities of 2π or π, respectively. Substituting $\theta(t)$ from Eq. (4) and using the identity

$$\exp[-i(\omega_1/\omega)\sin(\omega t)] = \sum_{p=-\infty}^{\infty} J_p(\omega_1/\omega)\exp(-ip\omega t) \tag{6}$$

yields

$$\mathscr{V}(\theta) = a_0/2 + \sum_{q=1}^{\infty} \sum_{p=-\infty}^{\infty} a_q J_p(q\alpha\omega_1/\omega) \times \cos[(p\omega - q\omega_n)t + q\alpha\theta_0] , \tag{7}$$

where $\omega_n = \alpha\omega_d$ is the measured fundamental frequency of the current oscillations.

The detailed conditions which determine when phase locking occurs depend upon the CDW's equation of motion. Since the precise form of this equation is uncertain, we will assume that phase locking occurs when the time-average pinning energy in the locked state is lower than in the unlocked state. From Eq. (7), the time-average pinning energy, $\langle \mathscr{V}(\theta) \rangle$, will be equal to $a_0/2$ unless $p\omega = q\omega_n$, in which case there is an additional polarization energy

$$\delta\langle \mathscr{V}(\theta_0) \rangle = \sum_n a_q J_p(q\alpha\omega_1/\omega)\cos(q\alpha\theta_0) , \tag{8}$$

where the sum is over all p and q such that $p/q = \omega_n/\omega$. Similarly, the time-average pinning force $\langle \mathscr{V}'(\theta) \rangle$ will be zero unless $p/q = \omega_n/\omega$, for which

$$\delta\langle \mathscr{V}'(\theta_0) \rangle = \sum_n (q\alpha) a_q J_p(q\alpha\omega_1/\omega)\sin(q\alpha\theta_0) . \tag{9}$$

The Fourier coefficients a_q in Eq. (5) are normalized so that $\max_\theta\{ | \sum_{q=1}^{\infty} (q\alpha) a_q \sin(q\alpha\theta) | \} = 1$. These equations are functions of θ_0 which, roughly speaking, characterizes the phase of the CDW oscillations due to dc current flow with respect to that of the applied ac current, and thus determines the coupling between them. For some range of θ_0, $-\theta_m < \theta_0 < \theta_m$, the polarization energy $\delta\langle \mathscr{V}(\theta_0) \rangle$ will be less than zero. Through variations of θ_0 over this range, the pinning force $\delta\langle \mathscr{V}'(\theta_0) \rangle$ can adjust to cancel changes in the dc electric field so that the effective force $\langle V_{\text{eff}} \rangle$, and therefore $\langle I_{\text{CDW}} \rangle$, remain constant. Since the extremal values of $\delta\langle \mathscr{V}'(\theta_0) \rangle$ occur at $\theta_0 = \pm\theta_m$ and since $\delta\langle \mathscr{V}'(\theta_0) \rangle$ is an odd function of θ_0, the width in voltage of the constant current step will be equal to $2V_M \delta\langle \mathscr{V}'(\theta_m) \rangle$. Note that if $\mathscr{V}'(\theta) = \sin\theta$, $\delta\langle \mathscr{V}(\theta_0) \rangle \neq 0$ only for $q = 1$ or $\omega_n/\omega = p$, i.e., no subharmonic steps are predicted. Subharmonic steps with $q > 1$ arise from the harmonics ($q > 1$) in the Fourier expansion of $\mathscr{V}'(\theta)$.

In order to calculate the widths of the steps in the dc I-V characteristic, some explicit form for the pinning potential must be assumed. We have chosen to use the nonsinusoidal potential previously proposed[10] within the context of the tunneling theory, and which was discussed in paper I. The form of this potential is given by:

$$\mathscr{V}(\theta) \propto \begin{cases} -\cos\theta \quad \text{for } -\pi/2 < \theta < \pi/2 \pmod{2\pi} , & \text{(10a)} \\ \cos\theta \quad \text{for } \pi/2 < \theta < 3\pi/2 \pmod{2\pi} . & \text{(10b)} \end{cases}$$

The periodicity of the pinning is here π in phase, so that $\alpha = 2$ and $\omega_n = 2\omega_d$. Any potential having this general form—smooth minima separated by cusps—will yield similar results for the step widths. The maximum magnitude of the pinning force V_M was initially assumed to be equal to the dc threshold V_T.

Figure 9 shows the predicted step width versus ω_1/ω for the 1/1 step and several subharmonic steps. A comparison of these predictions with Fig. 2 shows that the major features of the experimental data are reproduced. In particular, the step size oscillates with ac amplitude, the envelope of the oscillations decreasing with increasing ac amplitude. Furthermore, the period of the oscillations with ac amplitude varies linearly with frequency and inversely with subharmonic order q, precisely as observed. However, the predicted amplitude of the subharmonic

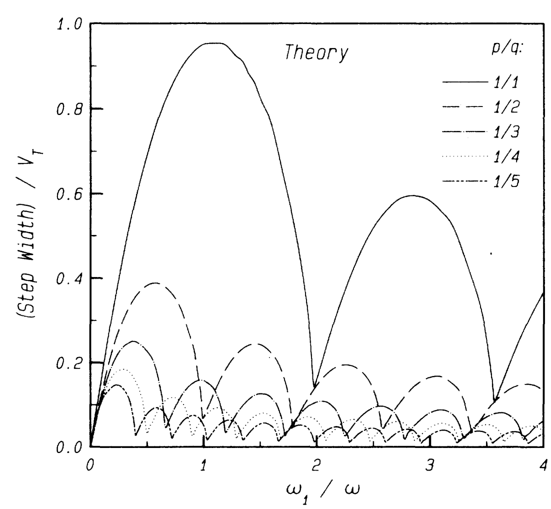

FIG. 9. Predicted widths of the 1/1 and several subharmonic steps in the dc I-V characteristic calculated using Eqs. (8), (9), and (10). The parameter ω_1/ω is the ratio of the applied ac current to the ac frequency.

steps is somewhat larger than is measured, especially for large q. Experimentally, the relative sizes of the smaller steps are reduced by rounding, which may result from the finite CDW velocity distribution within the crystal, from the finite lock-in probe amplitude, from noise, or from competition for locking on adjacent steps. More coherent samples exhibit somewhat larger subharmonic steps, and the oscillations of the step widths with ac amplitude are more pronounced. Even so, the decrease in the subharmonic step amplitudes for large q seems too great to be accounted for solely by these mechanisms. Since the calculation of the width of the p/q step involves only Fourier components of the pinning potential of order q and higher, this suggests that the actual potential is somewhat more rounded than that given in Eq. (10). The same conclusion was reached in paper I, based on an analysis of the current oscillation spectra.

The value of the parameter ω_1 may be deduced directly from the measured ac conductance, applied ac voltage, and ratio of the dc CDW current to the fundamental narrow-band noise frequency as

$$\omega_1 = (\omega_n / 2I_{\mathrm{CDW}}) G_{\mathrm{CDW}}(\omega, V_{\mathrm{ac}}, V_{\mathrm{dc}}) V_{\mathrm{ac}} \ . \tag{11}$$

Table II gives the values of ω_1/ω calculated directly from experiment at several frequencies, for the applied dc bias and ac amplitude which yielded the maximum width of the 1/1 step at each frequency. The measured ω_1/ω values are all very close to 1.1, in excellent quantitative agreement with the prediction in Fig. 9.

The predicted step sizes for the 1/1, 2/1, and 3/1 harmonic steps are shown in Fig. 10. The overall agreement with the experimental data shown in Fig. 3 is excellent. The initial increase in step size with ac amplitude becomes more gradual and the maximum step size decreases with increasing p. At large ac amplitudes, the envelope of the oscillations for different p is nearly identical, and the phase of the oscillations for even and odd p differ by 180°, as observed. The measured envelope decreases more rapidly with increasing ac amplitude than predicted, however.

One advantage of using the simple model discussed here is that it allows the basic processes involved in phase-locking to be easily understood. When the CDW is not phase-locked, the motion is quasiperiodic (i.e., the drift frequency ω_d is an irrational multiple of the applied ac frequency ω) and the time-average pinning force is very small. When phase locking occurs, the motion becomes periodic with period $T = 2\pi p/\omega_n = 2\pi q/\omega$. This periodic

TABLE II. Values of ω_1/ω at the maximum of the step width versus ac amplitude calculated directly from experiment, for ac frequencies of 2, 5, 10, and 20 MHz. The predicted value is 1.1. ($T = 121$ K.)

$\omega/2\pi$ (MHz)	ω_1/ω
2	1.02 ± 0.15
5	1.13 ± 0.15
10	1.13 ± 0.15
20	1.21 ± 0.15

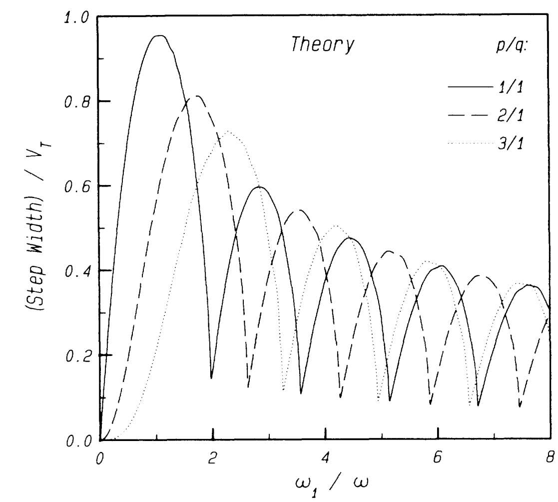

FIG. 10. Predicted widths of the 1/1, 2/1, and 3/1 harmonic steps versus ω_1/ω, calculated using Eqs. (8), (9), and (10).

modulation of the CDW's velocity by the ac field can then interfere constructively with that due to motion in the pinning potential. Thus, the CDW will dwell longer in certain parts of the potential than in others, resulting in a net time-average pinning force which depends upon the relative phases of the oscillations. On a step, the phases adjust to allow the pinning force to track changes in the applied electric field, thereby keeping the dc CDW current constant. The step size oscillates with ac amplitude because the amplitude determines how much and where the motion is retarded. For example, the first maximum in the width of the 1/1 step versus ac amplitude occurs when the CDW dwells in one part of the nth well of the potential, and then moves rapidly to the same part of the $(n+1)$th well. The second maximum occurs for an ac amplitude which carries the CDW back one well; the CDW "hops" from the nth well back to the $(n-1)$th well and then to the $(n+1)$th well and so on. As the ac amplitude is increased, the CDW hops between wells which are further and further apart. The amount of time spent moving slowly in a particular part of the potential thus decreases, so that the maximum pinning force and step width decrease. For a given step (p/q value), the ac frequency and the dc CDW drift velocity increase together. Thus, the ac amplitude required to reduce this velocity to near zero and achieve a given degree of locking must also increase with frequency.

This simple model is remarkably successful in accounting for all of our experiments, providing strong evidence that the pinning potential has the general form of Eq. (10). Nevertheless, some important quantitative discrepancies exist. First, a comparison of Figs. 2 and 3 with Figs. 9 and 10, respectively, shows that while the relative step sizes for different p/q values are adequately described, the absolute magnitudes of the observed step widths are considerably smaller than is predicted. For example, the maximum width of the 1/1 step measured at 20 MHz is approximately one-third of the predicted value. A similar discrepancy is also observed in the ac amplitude dependence of the dc threshold voltage (which corresponds to $p=0$ and $q=1$). As shown in Fig. 11, the predicted magnitude of the threshold-voltage oscillations is approximately four times larger than is measured at 20 MHz in Fig. 5. Furthermore, as discussed in paper I, the initial amplitude of the CDW voltage oscillations observed in response to a current pulse is smaller, by a similar factor, than expected. These discrepancies are much too large to be accounted for by experimental error or lack of sample coherence.

All of the above predictions of step sizes and oscillation amplitudes were made in terms of V_T, the dc threshold voltage measured in the absence of applied ac fields, since it was assumed that V_T reflects the maximum magnitude of the periodic pinning force. The most obvious explanation of our experimental results is that this is not quantitatively correct: the maximum magnitude of the periodic pinning force felt by a moving CDW is smaller, by roughly a factor of 3, than the measured dc threshold voltage. Several mechanisms may account for this. In the tunneling model, the dc threshold may not be determined by, and may be larger than, the maximum pinning force.[21] Alternatively, a distribution of pinning strengths may result in polarization processes which "bottleneck" the establishment of the current carrying state. These processes may become unimportant above threshold, or may not contribute to the periodically varying force. The observation of abrupt switching from zero to finite CDW current in impure $NbSe_3$ samples at low temperatures[18,22] and also the identification of switching centers[23] clearly indicates that localized defects can play an important role in determining the measured threshold voltage. Our observation that samples from a given growth tube with the most coherent response tend to have the lowest threshold fields also supports this idea. Furthermore, the dc threshold voltage is found to be independent of sample length in short samples,[24] indicating that contacts may play an important role as well.

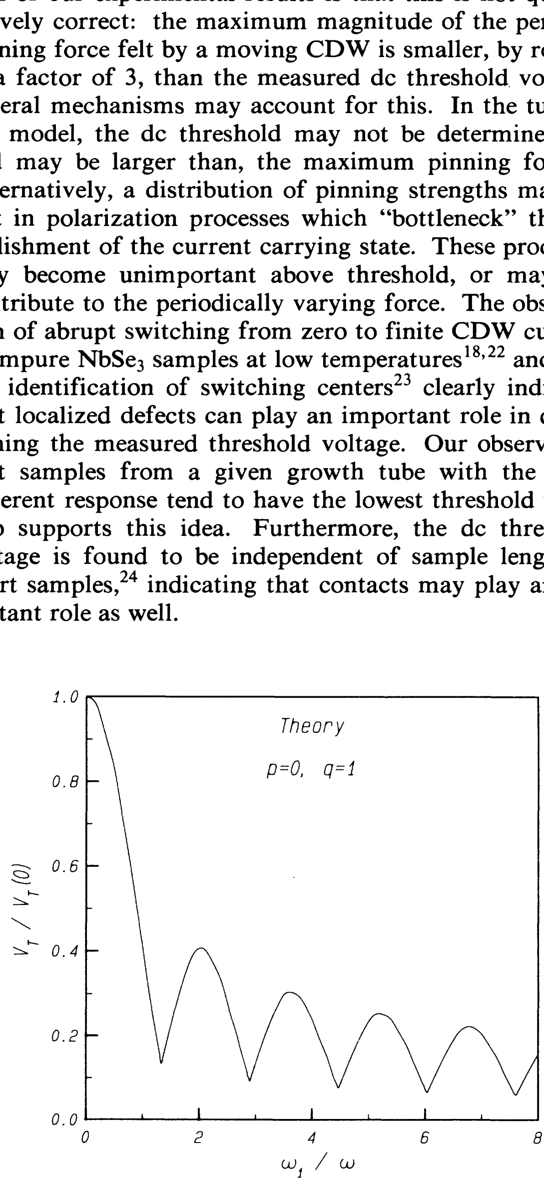

FIG. 11. Predicted variation of the dc threshold field with ω_1/ω. The amplitude of the oscillations is larger, by roughly a factor of 4, than is observed in Fig. 5.

A second quantitative discrepancy between our model and experiment is that the measured maximum step width as a function of ac amplitude is not independent of frequency. As seen in Fig. 4, the maximum step width increases rapidly with increasing frequency at low frequencies, but appears to saturate at high frequencies. The origin of this discrepancy is easily understood. As the ac frequency decreases, the steps in the I-V characteristic move closer and closer together. The maximum step width becomes limited by the spacing between the steps, and must tend to zero as the frequency is decreased. Related to this is the fact that the current-biased approximation used in our calculation breaks down at low frequencies. Previous simulations for Josephson junctions[20] indicate that a voltage-biased CDW should exhibit smaller steps than a current-biased CDW. The details of how the steps narrow as the frequency decreases depends upon the equation of motion for the system, and are not included within our model. These ideas may also account for the fact that measured step size generally decreases somewhat more rapidly with increasing ac amplitude than is predicted. A large ac voltage suppresses the dc nonlinearity, so that the steps move to smaller biases and become closer together with increasing ac amplitude.

As a second step in trying to understand our experimental results, we have performed extensive computer simulations of phase-locking phenomena. We chose to simulate the simple equation of motion motivated by the tunneling theory which was discussed in paper I. Assuming that acceleration due to Zener tunneling of CDW electrons is determined by the difference between the applied electric force and the effective pinning force, the CDW current may be written as

$$I_{\mathrm{CDW}}(t)=G_b V_{\mathrm{eff}}\exp(-V_0/V_{\mathrm{eff}}) , \tag{12}$$

where $V_{\mathrm{eff}}(t)=V(t)-V_M\mathscr{V}'(\theta)$, $V(t)=V_{\mathrm{dc}}+V_{\mathrm{ac}}\cos(\omega t)$, and $I_{\mathrm{CDW}}(t)\propto d\theta/dt$. We assume the same form for the pinning potential in Eq. (10), and, for reasons discussed above, take $V_M=\frac{1}{3}$. This simple first-order differential equation for $\theta(t)$ yields an excellent fit to the dc I-V characteristic and also accounts for the current oscillation spectra measured in $NbSe_3$. Aside from the maximum pinning force, all parameters used in the simulations were obtained from a fit to the dc I-V characteristic and from measurements of the current oscillations, and are given in Table I. We note that the qualitative features of the simulations do not depend crucially on the choice of this particular equation of motion. The rigid overdamped oscillator equation with a potential of the form given in Eq. (10) yields similar results, although the predicted shape of the dc I-V characteristic and thus the position of the steps on the voltage scale agree poorly with experiment.

Figure 12 illustrates the predicted behavior of the dc CDW current, pinning force, and pinning energy in the vicinity of the 1/1 step. As assumed in our previous calculation, the time-average pinning force is seen to vary linearly on a step to cancel changes in the dc bias. The time-average pinning energy is lowered when phase-locking occurs, and varies approximately quadratically on a step. In the unlocked regions adjacent to the step, the motion is erratic: the CDW drift velocity averaged over one cycle of the applied ac voltage slowly asymptotes to the locked value and then suddenly diverges away from it. This behavior is responsible for an increased slope of $\langle I_{\mathrm{CDW}} \rangle$, producing the negative "wings" in dV/dI at the edge of a step which are seen, for example, on the 1/1 and 1/2 steps in Fig. 1. This behavior also increases the time-average pinning energy. Phase locking thus becomes energetically favorable for a wider range of dc biases, so that the predicted step widths are now slightly larger than would be expected from our previous calculation.

The calculated maximum width of the 1/1 step versus ac frequency is compared with experiment in Fig. 13. Although the calculated width is found to increase at low frequencies and saturate at high frequencies, the saturation occurs much more rapidly than is observed. Rounding of the steps is experimentally more important at low frequencies (which correspond to biases near threshold) because the CDW velocity distribution is larger and the step widths are smaller. Fluctuations and metastable transitions in the depinned CDW, which are evident in current oscillation measurements at biases near threshold and which appear to be associated with the crystal defects responsible for the velocity distribution, may also lead to increased rounding and smaller observed step widths at low frequencies.

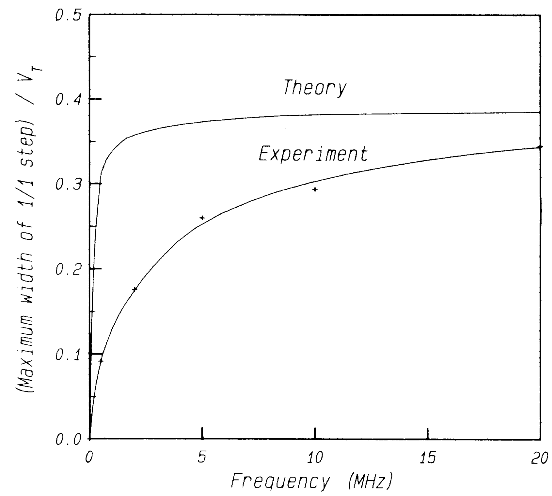

FIG. 13. Comparison of predicted and measured maximum widths of the 1/1 step vs ac frequency.

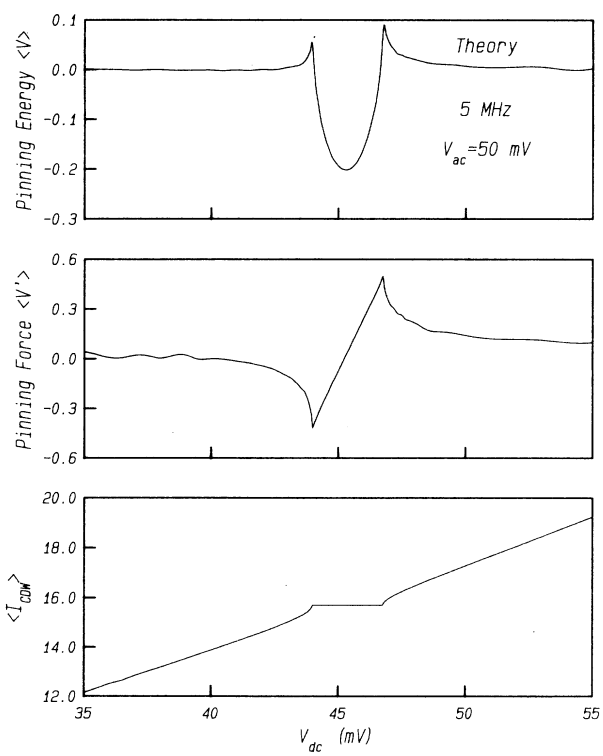

FIG. 12. Predicted CDW current, time-average pinning force, and time-average pinning energy near the 1/1 step, calculated using Eqs. (10) and (12). The pinning energy is lowered (i.e., the CDW becomes more strongly pinned) when phase locking occurs, and the pinning force varies linearly to cancel changes in the applied dc bias, thereby keeping the dc CDW current constant.

We have also used Eq. (12) to calculate the bias-dependent ac conductance of the CDW. This equation is obviously deficient, because the vanishing of Zener tunneling at low fields here implies that the small-signal zero-bias ac conductivity is extremely small at all frequencies. In the complete tunneling theory, CDW acceleration by an ac field occurs via photon-assisted tunneling (PAT), which is not included in this simple model; at high frequencies, PAT leads to a small-signal zero-bias ac conductance which approaches the limiting high-field dc conductance. Nevertheless, for dc biases above threshold and/or large ac amplitudes, Eq. (12) should represent a reasonable first approximation. Figure 14 shows the calculated bias-dependent ac conductance at 5 MHz for four different ac amplitudes. Because the simulations are extremely time consuming, we have performed detailed calculations only near the 1/1 and 1/2 steps. A comparison with Fig. 8 shows that all qualitative features of experiment are excellently reproduced. At small ac amplitudes, sharp jumps in ReG and large negative dips in ImG are predicted. As the ac amplitude is increased, these features become more rounded and vanish at large ac amplitudes. Even the positive "capacitive" bump observed in ImG at moderate amplitudes is reproduced. Differences between the predicted and measured sharpness of the features may result from the finite velocity distribution within the crystal, from instrumental noise, or from CDW fluctuations. In any case, sharp features are indeed observed in some samples. The apparent "inductive" and "capacitive" behavior is associated with the variations in the phase of the dc current oscillations relative to that of the ac voltage, which are required in order to achieve phase locking at different ac amplitudes. The phase and the ac amplitude together determine in what parts of the cycle the pinning force accelerates and retards the motion, and thus determine whether the ac current leads or lags the voltage. The detailed behavior depends upon the form of the pinning potential. Thus, the remarkable correspondence between the

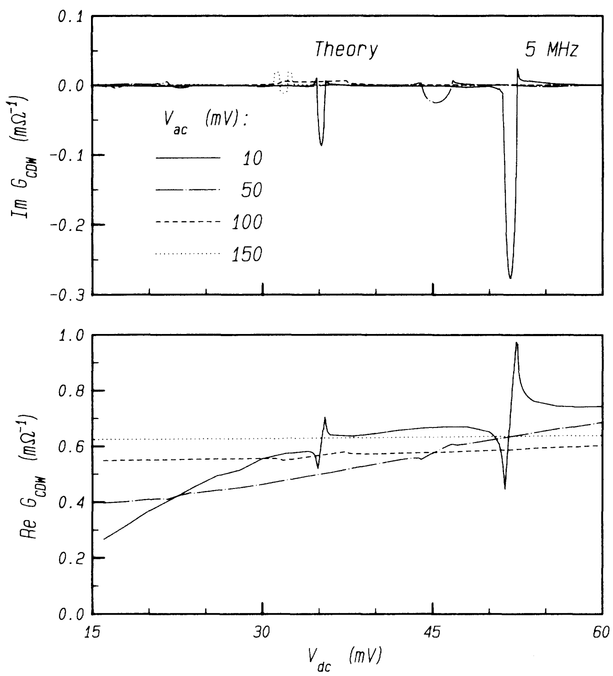

FIG. 14. Predicted bias-dependent ac conductance at 5 MHz for peak ac voltages of 10, 50, 100, and 150 mV, calculated using Eqs. (10) and (12). Detailed calculations were performed only near the 1/1 and 1/2 interference features. The measured "inductive" and "capacitive" features in $\mathrm{Im}\,G_{\mathrm{CDW}}$ and the jumps in $\mathrm{Re}\,G_{\mathrm{CDW}}$ seen in Fig. 8 are reproduced.

predictions of Fig. 14 and the data of Fig. 8 provides strong evidence for CDW motion in a pinning potential of the general form given in Eq. (10). It should be emphasized that the complete PAT model has previously been shown[25] to accurately reproduce all the experimental features of the bias-dependent ac conductivity seen in Fig. 8, except for the interference features. A simulation incorporating both aspects of the CDW dynamics would therefore be expected to yield an accurate description of experiment under all conditions.

The simple model which we have used here also accounts for other features of the CDW response. Steps in the dc I-V characteristic of $NbSe_3$ induced by rectangular-wave rather than sine-wave drives have been studied.[26] Quantitative discrepancies were found between the measured step size and its dependence on the on and off times of the drive when compared with the predictions of the rigid overdamped oscillator model of Eq. (2). The origin of these discrepancies was illustrated in Table II of paper I: the parametrization of experiment provided by the rigid ODO model is highly inconsistent. However, this obviously does not rule out the possibility of a single-coordinate description; we believe that the simple model discussed here can reproduce all of the observed results.

Interference phenomena have also been observed in the elastic response of the CDW's in $NbSe_3$ and TaS_3.[7] For applied dc and ac electric fields such that steps are observed in the dc I-V characteristic, Young's modulus increases and the internal friction decreases toward the values observed below threshold. These observations are easily understood. When phase locking occurs, the time-average pinning energy increases, so that the CDW becomes more strongly pinned to the lattice than in the unlocked state. The increase in pinning energy is roughly proportional to the width of the step, and decreases rapidly with increasing subharmonic order q. Thus, on a phase-locked step Young's modulus and the internal friction should tend to the pinned values observed below threshold, and the size of the anomalies should decrease with increasing q, precisely as is observed.

Tessema and Ong[27] have studied the CDW response to large-amplitude ac voltages below the second $NbSe_3$ transition using phase-space plots of the time-varying current versus voltage. For ac amplitudes below threshold, the observed Lissajous-like loops rotated clockwise, indicative of capacitive behavior. As the ac amplitude was increased above threshold, inductive (counterclockwise-rotating) end loops appeared, and at large ac amplitudes the loops opened up and became fully inductive. Increasing the ac frequency was found to greatly enhance the hysteresis. Such behavior is characteristic of inertial systems. Using an equation of motion similar to that of the ODO model of Eq. (2) but including a finite CDW mass, Tessema and Ong were able to obtain reasonable qualitative agreement with experiment by assuming values for $\omega/\omega_{\mathrm{co}}$ roughly an order of magnitude larger than those experimentally observed. The origin of this discrepancy is twofold. First, below the second CDW transition in $NbSe_3$, the peak in the imaginary part of the ac conductivity, and therefore ω_{co}, is skewed to higher frequency by the contribution of the CDW which forms below the first transition. Second, as discussed previously, the parametrization of experiment provided by the ODO model is inconsistent. As a result, use of the measured ω_{co} and V_T values yields predicted CDW displacements in the presence of an applied sinusoidal voltage which are roughly 10 to 15 times greater than those which actually occur, and which are therefore appropriate to a much lower applied frequency. Figure 15 shows plots of the time-varying current versus voltage for two ac frequencies $f=\omega/\omega_{\mathrm{co}}$, calculated by inserting the pinning potential of Eq. (10) in the (massless) overdamped oscillator equation of Eq. (2).[28] As in Ref. 27, we have subtracted out the linear response. A comparison with Figs. 3 and 5 of Ref. 27 shows that all qualitative features of experiment are excellently reproduced. The apparent inductive or "inertial" behavior is a simple consequence of overdamped CDW motion in a periodic pinning potential.

Several other calculations of ac-dc interference phenomena in CDW systems have been made. Previous calculations[29,30] based on the classical elastic medium model yielded steps in the dc I-V characteristic and anomalies in the bias-dependent ac conductance. However, no subharmonic features were predicted, and the shapes of the anomalies do not agree very well with experiment. Subharmonic features were obtained using a strong-pinning model.[31] The applicability of such a model to $NbSe_3$ is uncertain, and the steps are predicted to vanish in large samples, in apparent disagreement with experi-

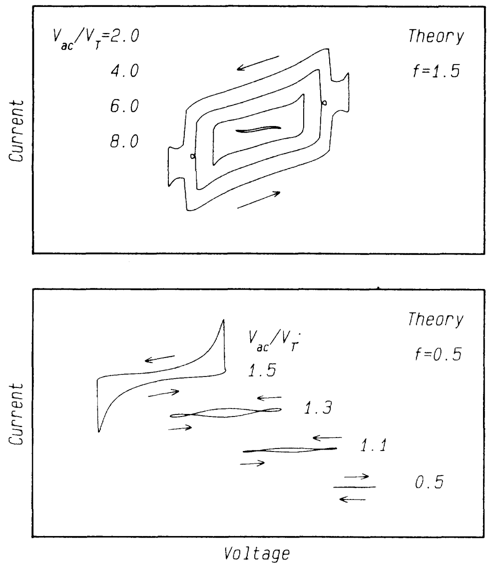

FIG. 15. Phase-space plots of current vs applied ac voltage for frequencies $f=\omega/\omega_{co}$ of 0.5 and 1.5, calculated using Eq. (2) with the pinning potential of Eq. (10).

ment. More recently, Coppersmith and Littlewood[32] have reported a detailed study of interference phenomena in the classical elastic medium model. Complete locking in dV/dI is predicted to occur only when the ac frequency and amplitude are small enough so that significant relaxation takes place while the field is below threshold. Complete locking and the negative "wings" in dV/dI mentioned earlier should not be observed for large frequencies and amplitudes, such that the time $\delta t \approx 2\pi V_T/\omega V_{ac}$ spent below threshold is small. Subharmonic features but not complete subharmonic locking are predicted, with the ratio of the widths of the 1/2 step to the 1/1 step scaling as $\omega^{-1/2}$ for large frequency and $V_{ac}^{-1/2}$ for large amplitudes. Unfortunately, specific estimates for the relevant voltage and frequency scales were not given.

Before comparing these predictions with experiment, it is important to understand the experimental factors which influence whether complete locking occurs. As emphasized in this paper and in paper I, any real crystal exhibits a distribution of time-average velocities which is associated with crystal defects and contact effects, and which is not accounted for in the classical elastic medium model. At a given applied dc bias, this distribution corresponds to a width δV in dc voltage. The "intrinsic" width of a step in the I-V characteristic is determined by the maximum time-average pinning force which can be developed. Complete locking will thus only be observed if the intrinsic step width is larger than δV corresponding to the velocity distribution. Heating effects are also important. Because a sample is nonuniformly heat-sunk along its length (with the best heat-sinking occurring at the contacts), ohmic heating for large applied fields results in thermal gradients, and thus in broadening of the velocity distribution within the crystal. The dc bias corresponding to a given step (p/q value) increases roughly linearly with the ac frequency at high frequencies. Further, the ac amplitude required to achieve a given step width (ω_1/ω value) increases linearly with frequency. Sample heating thus increases as the square of the frequency, and precludes the observation of complete locking at high frequencies. We have carefully characterized the velocity distribution in the $NbSe_3$ sample studied here through measurements of the spectral width of the narrow-band noise fundamental versus dc bias. Heating effects were quantified by comparing high-field dc and pulse I-V measurements. Thermal broadening of the velocity distribution limited our interference measurements to frequencies below 40 MHz.

In light of the above considerations, the predictions of Coppersmith and Littlewood[32] (CL) do not agree with experiment. First, as shown in Fig. 16, we observe complete locking in dV/dI on the 1/1 step for ac and dc fields such that the total applied field never goes below the zero-ac threshold field. Damped CDW relaxation below threshold is therefore *not* crucial to mode locking. The applied ac field need only retard and accelerate the motion in order to produce a nonzero pinning force, and therefore complete locking. Complete locking likely has not been observed previously under these circumstances because the samples used have not been sufficiently coherent; for small ac amplitudes the steps are narrow, so that a very narrow CDW velocity distribution is needed. Second, we observe complete subharmonic locking, as in the 1/2 and 1/3 steps in Fig. 1, for a broad range of frequencies and ac amplitudes, in clear disagreement with this model. (Complete subharmonic locking has also been observed by other groups.[11]) Together with the fact that the step widths oscillate with ac amplitude and frequency, it is not clear how CL's predictions for the relative widths of the 1/1 and 1/2 steps are to be interpreted. Third, we observe complete locking and "wings" in dV/dI for large ac voltages (above 20 V_T) and frequencies (30 MHz), such that

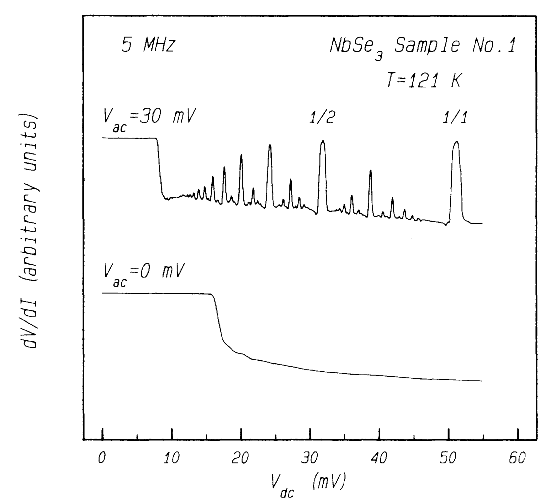

FIG. 16. Differential resistance measured in the presence of a 5-MHz, 30-mV peak ac voltage. The 1/1 step locks completely even though the total voltage never goes below the zero-ac dc threshold.

the time δt which the CDW spends relaxing below threshold is equal to that of the experimental data of Fig. 1 of Ref. 32, which is within the stated regime of validity of CL's calculation. Furthermore, the maximum completely locked width of the 1/1 step was observed at 20 MHz (heating effects were important at higher frequencies), which is greater than the classical crossover frequency of this sample. Even when incomplete locking was observed, it was always consistent with the CDW velocity distribution deduced from measurements of the current oscillations. All significant predictions of the classical elastic medium model contained in Ref. 32 are thus found to be in direct contradiction with our experiments.

IV. CONCLUSION

In this paper, we have presented a detailed experimental study of ac-dc interference phenomena in charge-density-wave transport. These qualitative effects are typical of nonlinear systems with competing periodicities; direct analogs are observed in the classical motion of a pendulum within a gravitational field and also in the interference between macroscopic quantum states in Josephson junctions. We have analyzed our results using a simple single-coordinate model, motivated by the tunneling theory, for a CDW moving in a nonsinusoidal potential. Use of this model leads to a very simple and transparent interpretation of the basic physics involved in phase locking. Further, it provides an excellent semiquantitative account of all of the observed phenomena, including the steps in the dc I-V characteristic, the jumps and inductive dips in the bias-dependent ac conductance, the anomalies observed in the elastic response, and the inductive loops observed in phase-space plots of the CDW's response to ac fields. Together with our measurements of current oscillations, these results provide strong evidence that the CDW's interaction with impurities may be described, to good approximation, by a periodic pinning potential of the general form given in Eq. (10).

Our results are not, on the other hand, consistent with predictions derived from the classical elastic medium model. Although those predictions reproduce some very general qualitative features of the observed response, this does not, as has been suggested, constitute significant evidence for the validity of the classical model. Indeed, given the extremely general nature of the interference phenomena, it would be remarkable only if such effects did not occur at all within that framework. The detailed predictions of Coppersmith and Littlewood[32] for ac-dc interference are unambiguously contradicted by our experiments. Our experiments and analysis clearly establish that the most important features of the current oscillation and interference phenomena can be accurately described in terms of a simple single-coordinate model.

ACKNOWLEDGMENTS

We wish to thank J. Hubacek, G. Gammie, J. H. Miller, Jr., G. Mozurkewich, S. E. Brown, and L. Mihály for fruitful discussions and S. Skala for providing technical assistance. This work was funded by the U.S. Joint Services Electronics Program (under Contract No. N00014-84-C-0149) and by the National Science Foundation (under Grant No. NSF-DMR-83-16981).

[1]H. Fukuyama and P. A. Lee, Phys. Rev. B **17**, 535 (1978); P. A. Lee and T. M. Rice, *ibid.* **19**, 3970 (1979).

[2]R. E. Thorne, W. G. Lyons, J. W. Lyding, J. R. Tucker, and John Bardeen, preceding paper, Phys. Rev. B **35**, 6348 (1987).

[3]P. Monceau, J. Richard, and M. Renard, Phys. Rev. Lett. **45**, 43 (1980).

[4]A. Zettl and G. Grüner, Solid State Commun. **46**, 501 (1983).

[5]S. Shapiro, A. Janus, and S. Holly, Rev. Mod. Phys. **36**, 223 (1964).

[6]A. Zettl and G. Grüner, Phys. Rev. B **29**, 755 (1984).

[7]L. C. Bourne, M. S. Sherwin, and A. Zettl, Phys. Rev. Lett. **56**, 1952 (1986).

[8]J. Richard, P. Monceau, and M. Renard, Phys. Rev. B **25**, 948 (1982).

[9]R. E. Thorne, J. R. Tucker, John Bardeen, S. E. Brown, and G. Grüner, Phys. Rev. B **33**, 7342 (1986).

[10]John Bardeen, in *Highlights of Condensed Matter Theory,* Proceedings of the International School of Physics "Enrico Fermi", Course LXXXIX, edited by F. Bassani, F. Fumi, and M. Tosi (North-Holland, Amsterdam, 1985), p. 349.

[11]S. E. Brown, G. Mozurkewich, and G. Grüner, in *Charge Density Waves in Solids,* edited by Gy. Hutiray and J. Sólyom (Springer-Verlag, Berlin, 1985), p. 318; M. S. Sherwin and A. Zettl, Phys. Rev. B **32**, 5536 (1985).

[12]A. Zettl (unpublished).

[13]W. G. Lyons, R. E. Thorne, J. H. Miller, Jr., and J. R. Tucker, Phys. Rev. B **31**, 6797 (1985).

[14]G. Grüner, W. G. Clark, and A. M. Portis, Phys. Rev. B **24**, 3641 (1981).

[15]P. Monceau, J. Richard, and M. Renard, Solid State Commun. **41**, 609 (1982).

[16]W. C. Stewart, Appl. Phys. Lett. **12**, 277 (1968); D. E. McCumber, J. Appl. Phys. **39**, 3113 (1968).

[17]S. Sridhar, D. Reagor, and G. Grüner, Phys. Rev. Lett. **55**, 11 (1985).

[18]P. Monceau, J. Richard, and M. Renard, Phys. Rev. B **25**, 931 (1982).

[19]G. Grüner, A. Zawadowski, and P. M. Chaikin, Phys. Rev. Lett. **46**, 511 (1981).

[20]P. Russer, J. Appl. Phys. **43**, 2008 (1972); M. J. Renne and D. Polder, Rev. Phys. Appl. **9**, 25 (1974); J. R. Waldram and P. H. Wu, J. Low Temp. Phys. **47**, 363 (1982); P. Bak, in Proceedings of the International Symposium on Nonlinear Transport and Related Phenomena in Inorganic Quasi-One-Dimensional Conductors, Sapporo, Japan, 1983 (unpublished).

[21]In the tunneling model, the threshold field is determined by the requirement that electrons pick up sufficient energy from the field to overcome the pinning gap in a distance $2L_d$, twice the Lee-Rice domain length. This gives $2eE_TL_d = E_g = 2v_F/L_d$, twice the π-soliton energy.

[22]A. Zettl and G. Grüner, Phys. Rev. B **26**, 2298 (1982); M. P. Everson and R. V. Coleman, *ibid.* **28**, 6659 (1983).

[23]R. P. Hall, M. F. Hundley, and A. Zettl, Phys. Rev. Lett. **56**, 2399 (1986).

[24]J. C. Gill, Solid State Commun. **44**, 1041 (1982); G. Mihály, Gy. Hutiray, and L. Mihály, Phys. Rev. B **28**, 4896 (1983); G. Mihály, Gy. Hutiray, and L. Mihály, Solid State Commun. **48**, 203 (1983).

[25]R. E. Thorne, W. G. Lyons, J. H. Miller, Jr., J. Richard, and J. R. Tucker, Solid State Commun. **50**, 833 (1984).

[26]S. E. Brown, G. Grüner, and L. Mihály, Solid State Commun. **57**, 165 (1986).

[27]G. X. Tessema and N. P. Ong, Phys. Rev. B **31**, 1055 (1985).

[28]Use of Eq. (12) instead of the overdamped-oscillator equation [Eq. (2)] yields similar qualitative features; however, the vanishing of the Zener force distorts the shape of the loops at small ac voltages. A more realistic calculation should include CDW acceleration by photon-assisted tunneling.

[29]L. Sneddon, M. C. Cross, and D. S. Fisher, Phys. Rev. Lett. **49**, 292 (1982); L. Sneddon, Phys. Rev. B **29**, 725 (1984); L. Sneddon, Phys. Rev. Lett. **52**, 65 (1984).

[30]S. N. Coppersmith and P. B. Littlewood, Phys. Rev. B **31**, 4049 (1985).

[31]P. F. Tua and J. Ruvalds, Solid State Commun. **54**, 471 (1985).

[32]S. N. Coppersmith and P. B. Littlewood, Phys. Rev. Lett. **57**, 1927 (1986).